

Fig. 1 Change of magnetic induction  $B$  with temperature below and above the Curie temperature for a material that is ferromagnetic below the Curie temperature.

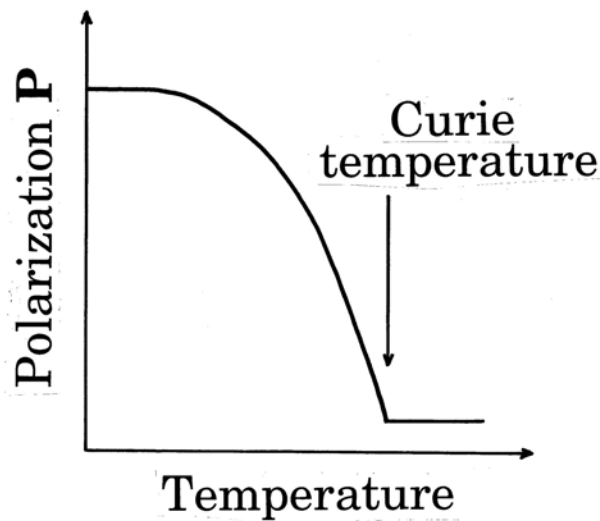


Fig. 2 Change of polarization  $P$  with temperature below and above the Curie temperature for a material that is ferroelectric below the Curie temperature.

There are also solid-solid phase transitions that involve a change in the arrangement of the electric dipoles, as the change of a ferroelectric phase to a paraelectric phase upon heating past the dielectric Curie temperature. The relative permittivity  $\epsilon_r$  is much higher for the ferroelectric phase than a paraelectric phase, so the polarization  $P$  decreases upon heating past the Curie temperature (Fig. 2). At the Curie temperature, the communication among the unit cells to line up their electric dipoles vanishes.

Moreover, there are solid-solid phase transitions that involve the change of a superconducting phase to a normal (conducting) phase upon heating past the superconducting critical temperature  $T_c$ . Above  $T_c$ , superconductivity vanishes, and the

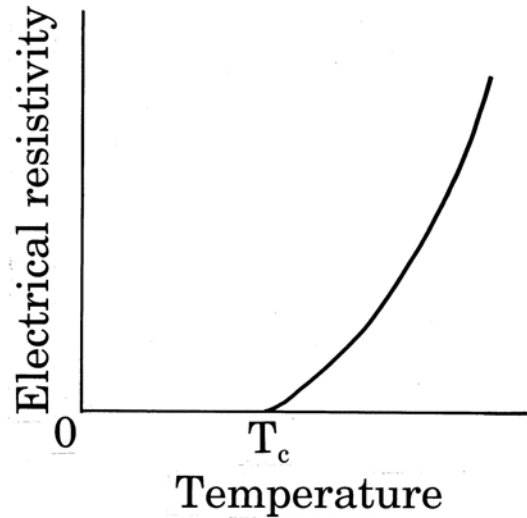


Fig. 3 Change of the volume electrical resistivity with temperature below and above the superconducting critical temperature  $T_c$  for a material that is superconducting below  $T_c$ .

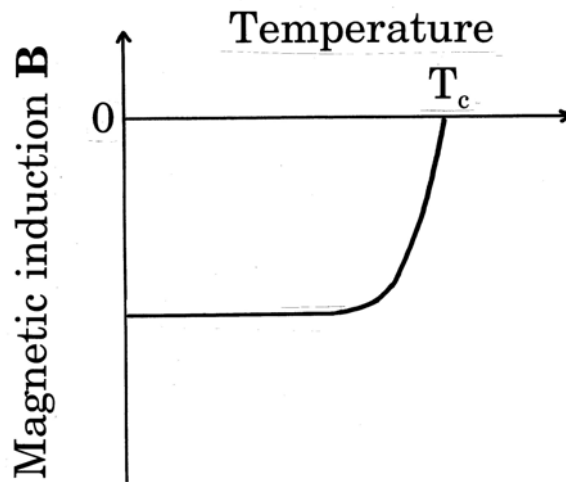


Fig. 4 Change of magnetic induction  $\mathbf{B}$  with temperature below and above the superconducting critical temperature  $T_c$  for a material that is superconducting (exhibiting the Meissner Effect) below  $T_c$ .

material becomes a normal conductor. Thus, the volume electrical resistivity is zero below  $T_c$  but is non-zero above  $T_c$ , as shown in Fig. 3. As superconducting phase is strongly diamagnetic, i.e., the magnetic dipole moment in a superconductor is in a direction opposite to the applied magnetic field. This exceptionally strong diamagnetism (much stronger than the diamagnetism in copper or other conventional diamagnetic materials) causes a superconductor to repel a magnet. This phenomenon is known as the Meissner Effect. Fig. 4 illustrates the decrease of the magnitude of the negative  $\mathbf{B}$  ( $\mu_r < 0$ ) as the temperature is increased to  $T_c$ .

In general, a phase transition that is reversible may be used as the basis for smart behavior, as a change in temperature past the phase transition temperature serves as the stimulus for a large change in a certain property, whether magnetic, dielectric, electrical, optical, mechanical, thermal or other properties. When the temperature changes back to the initial value, the property also changes back to the initial value. The reversibility enables the device to be used more than once. (If the phase transition is irreversible, the device can be used only once.)

A phase transition does not have to occur at one temperature, as it can, in some cases, occur over a range of temperatures. For example, FCC iron (also called austenite) containing a small amount of carbon as an interstitial solute, upon fast cooling, transforms to a body-centered tetragonal (BCT) phase of the same composition. The BCT phase is called martensite. This solid-solid phase transition is called the martensitic transformation. It occurs over a range of temperatures – from  $M_s$  (start of martensitic transformation upon cooling) to  $M_f$  (finish of martensitic transformation upon cooling). At a temperature between  $M_s$  and  $M_f$ , the martensitic transformation is not complete and austenite coexists with martensite, for however long this temperature is maintained. To obtain 100% martensite, the temperature must be lowered below  $M_f$ . The extent of martensitic transformation is not controlled by the time, but by the temperature. The martensitic transformation is said to be athermal. That time does not affect the extent of the martensitic transformation is because the transformation does not involve the diffusion of atoms (i.e., it is diffusionless). There is no long-distance diffusion, which occurs in the case of a eutectoid transformation. Atoms move cooperatively in a shear deformation. Austenite and martensite have the same composition (% carbon).

A phase transition does not have to involve a change of a thermodynamically stable phase to another thermodynamically stable phase. (A thermodynamically stable phase is one which has the lowest energy, as the lowest energy state is the stable state.) An example of a change of a stable phase to another stable phase is the melting of ice, as ice is the stable phase below 0°C (at 1 atm) and water is the stable phase above 0°C. On the other hand, the martensitic transformation involves the change of an unstable phase (austenite) to a metastable phase (martensite). Just above  $M_s$ , austenite is unstable (austenite is stable at much higher temperatures), and would transform to stable phases (BCC iron called ferrite, together with  $Fe_3C$ , called cementite) if thermal energy and time are sufficient. However, upon fast cooling, both thermal energy and time are insufficient (i.e., the time spent at temperatures that provide enough thermal energy for atoms to move is too short), so the change of the unstable austenite to the stable phases is suppressed. It is only when the change to the stable phases is not possible that the change to the metastable phase is possible. A metastable phase does not have as low an energy as the stable phase, but it has a lower energy than the unstable phase. Upon subsequent heating, a metastable phase will change to the stable phase(s), as the heating provides the thermal energy and time for the transformation. In the case of the martensite, it changes to the stable phases (ferrite + cementite) upon heating above  $M_s$ , provided that the time of heating is sufficient, as atom movement (by diffusion in this case) takes time. Diffusion is involved in the change of martensite to ferrite + cementite, because martensite, ferrite and cementite all have different compositions. Ferrite is the least rich in carbon; cementite is the richest in carbon; martensite is in between. Hence, during the phase

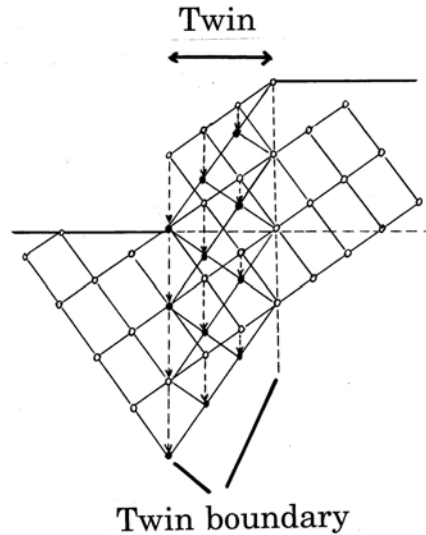


Fig. 5 Twinning forming two twin boundaries (mirror planes) between which is a twin.

change, the carbon atoms have to diffuse toward the cementite being formed and iron atoms have to diffuse toward the ferrite being formed.

## 2. The shape-memory effect

The shape-memory effect [1-3] refers to the ability of a material to transform to a phase having a twinned microstructure that, after subsequent plastic deformation, can return the material to its initial shape when heated. Twinning involves the movement of atoms so that the atom positions at either side of a twin boundary are mirror images of one another (Fig. 5). The initial phase is body-centered cubic and is called austenite (even when it is not an iron-based alloy). The highly twinned phase to which austenite transforms is called martensite (even when it is not BCT and not an iron-based alloy). Martensite generally has less crystallographic symmetry than austenite. However, the twinning enables plastic deformation (typically as much as 8%) to occur easily. Austenite begins to transform to martensite at temperature  $M_s$  upon cooling and the transformation is completed upon further cooling to temperature  $M_f$ . Deformation is applied to the martensite. It can occur through either the growth of favorably oriented twins or deformation twinning (twinning upon shear during deformation). Upon unloading and subsequent heating, martensite transforms back to austenite through reversal of the deformation mechanisms involving twinning and the shape recovers. Martensite begins to transform to austenite upon heating at temperature  $A_s$  and the transformation is completed upon further heating to temperature  $A_f$ . In general,  $M_f < M_s < A_s < A_f$ . The shape-memory transformation is reversible but has a large hysteresis.

The shape-memory effect is illustrated in the crystal lattice level in Fig. 6. If the shape-memory alloy (SMA) is constrained from recovering (say, within a composite material), a recovery stress is generated. The recovery stress builds up upon heating the martensite and it increases with increasing prior strain of the martensite. The stress-strain curve of an SMA at temperatures below  $A_s$  (i.e., for martensite) is shown in Fig. 7(a).

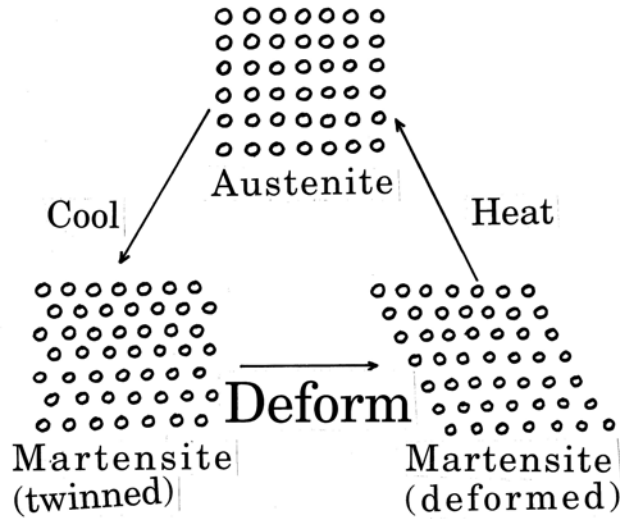


Fig. 6 The shape-memory effect illustrated in the crystal lattice level.

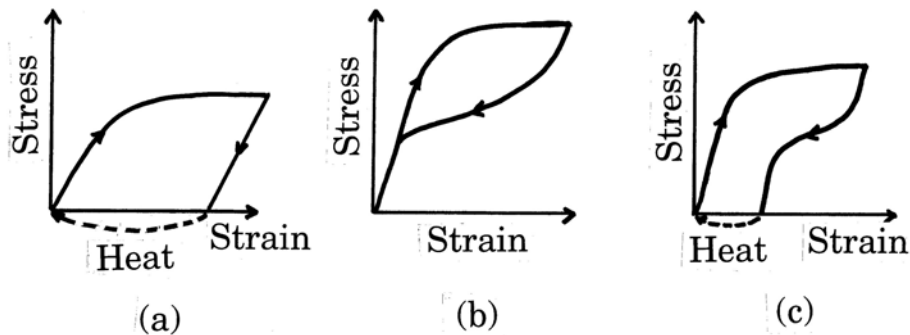


Fig. 7 Stress-strain curve of an SMA at temperature  $T$ . (a)  $T < A_s$ , (b)  $T > A_f$ , (c)  $A_s < T < A_f$ .

The curve shows the deformation. The arrow marked “heat” shows the strain (shape) recovery upon subsequent heating. The strain recovery upon heating means the conversion of thermal energy to mechanical work.

The martensitic transformation in an SMA is different from that in the Fe-C system (Sec. 1) in that it is thermoelastic. This means that the martensite crystals grow at a velocity proportional to the cooling rate and shrink when heat is applied. This is in contrast to the athermal nature of the non-thermoelastic martensitic transformation of the Fe-C system, in which the martensite crystals grow quickly to their final size. In order for a thermoelastic transformation to occur, both the interface energy (energy of the interface between the martensite phase and the parent phase) and the energy needed by the plastic deformation must be small. During the thermoelastic martensitic transformation, the interface between the parent phase and the martensite remains coherent (i.e., the atom planes bend slightly and continue across the interface, rather than ending at the interface (Fig. 8)) while it moves.

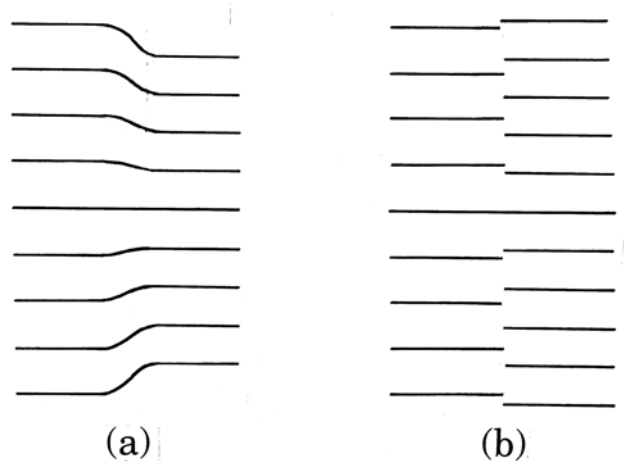


Fig. 8 (a) A coherent interface (with the bending of atom planes exaggerated).  
 (b) An incoherent interface.

Most SMA's have superlattice structures where the fundamental lattices are BCC and are classified as  $\beta$ -phase alloys. The martensitic transformation involves twinning (shearing) in the  $[\bar{1}10]$  direction along the (110) plane (the habit plane) of the parent phase and results in an orthorhombic martensite. An SMA alloy AB exhibits the CsCl structure (i.e., a cubic unit cell with Cl atoms at the corners and Cs atom at the body center) and is denoted  $\beta_2$ . An SMA alloy  $A_3B$  exhibits the  $Fe_3Al$  structure (i.e., a cubic unit cell with Al atoms at the corners and face centers and the Fe atoms at the body center of the cube, at the mid-point of every edge of the cube and at the body center of each of eight quadrants of the cube) and is denoted  $\beta_1$ . Even though the parent phase may be a single crystal, a number of martensites with different but crystallographically equivalent habit planes may be formed in different parts of the specimen. These martensites are called variants. The formation of a single variant may be promoted by cooling from one end of the specimen and letting the variant grow from that end.

SMA's most commonly exhibit one-way shape memory i.e., the transformation to the desired shape occurs only upon heating, i.e., the memory is with the parent phase. However, some SMA's (e.g., Ni-Ti, Cu-Al, In-Tl and Fe-Mn-C) exhibit two-way shape memory, in that the deformed shape is remembered during cooling, in addition to the original shape being remembered during heating, i.e., the memory is with both parent and martensite phases. The remembering of the deformed shape during cooling occurs by the forming of favorably oriented twins during cooling between  $M_s$  and  $M_f$ . This requires subjecting the SMA to training, which entails a sufficient number (say 100) of shape memory cycles involving the same deformation process and strain.

The martensitic transformation may be induced by stress rather than by temperature. This makes sense because the martensitic transformation involves twinning, which occurs under shear. Beyond a certain stress, martensite starts to form from austenite and results in elastic elongation that exceeds the elasticity of ordinary alloys by a factor of 10 or more. Upon removal of the stress, the martensite changes back to austenite and the strain (shape) returns to the value prior to the martensitic transformation. This phenomenon occurs above  $A_f$  (i.e., for austenite) and is known as

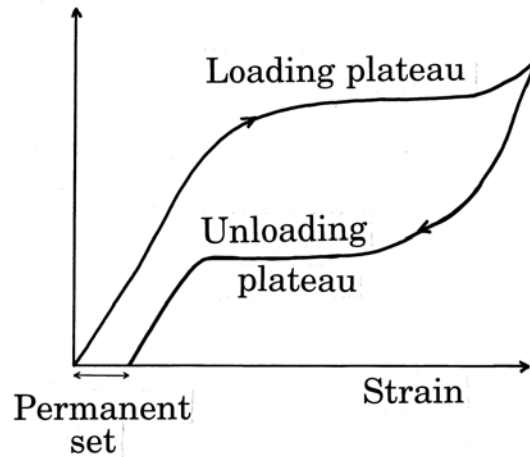


Fig. 9 Stress-strain curve of an SMA at temperature  $T > A_f$ , showing a permanent set after unloading.

superelasticity (or pseudoelasticity). It is illustrated in Fig. 7(b), where the stress has a plateau during loading and another plateau during unloading. Typically, a strain of 10% can be nearly fully recovered, out of which a strain of about 8% is due to the stress induced martensitic transformation and the rest is due to conventional elasticity. As shown in Fig. 7(b), a superelastic material does not follow Hooke's Law, but gives a nearly constant stress (the plateau) when strained typically between 1.5% and 7%. The near constancy of the stress during unloading is exploited in orthodontal braces, where an SMA is used for the archwire, which applies forces according to the unloading plateau in order to restore the teeth to their proper location.

The large hysteresis between loading and unloading in Fig. 7(b) means that a significant part of the strain energy put into the SMA is dissipated as heat. This energy dissipation provides a mechanism for vibration damping. Furthermore, the motion of the coherent interfaces between martensite and austenite occurs quite easily under small stresses, thus causing the absorption of vibrational energy. As a result, SMA's tend to have excellent damping ability [4].

Fig. 7(b) shows the strain to be totally reversible. However, in some cases (especially if the strain is large), there can be a small permanent set (non-zero strain) after complete unloading, as shown in Fig. 9.

Fig. 7(a) and (b) differ in that (i) the former applies to martensite (below  $A_s$ ) and the latter applies to austenite (above  $A_f$ ) and (ii) the former involves strain (shape) recovery with heat and the latter involves recovery without heat. At temperatures between  $A_s$  and  $A_f$ , Fig. 7(c) applies; Fig. 7(c) exhibits attributes from both Fig. 7(a) and (b).

The most common SMA is Ni-Ti (53-57 wt.% Ti), called 55-Nitinol because it contains Ni, Ti and was first studied in Naval Ordnance Laboratory. Other SMA's include copper-based alloys such as Cu-Zn, Cu-Zn-Al, Cu-Zn-Ga, Cu-Zn-Sn, Cu-Zn-Si, Cu-Al-Ni, Cu-Au-Zn and Cu-Sn, in addition to Au-Cd, Ni-Al and Fe-Pt. The main competition is between NiTi and CuZnAl. NiTi has better performance, but CuZnAl costs less. In order to avoid strain that cannot be recovered through the shape-memory



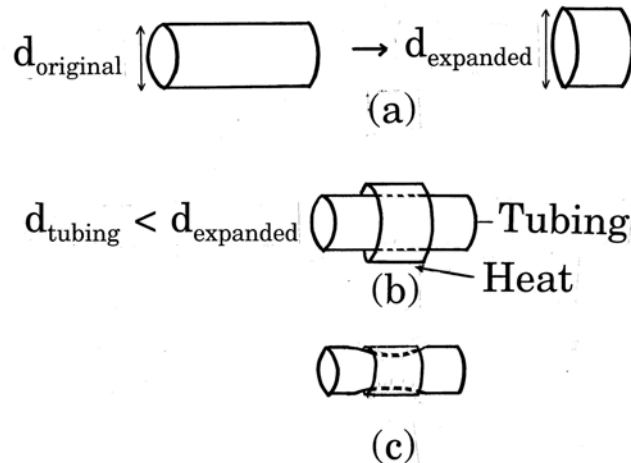


Fig. 10 The use of a shape-memory alloy for coupling tubing.

effect, the strain should be below 6% for NiTi and below 2% for CuZnAl. Both alloys have transformation temperatures in the range between  $-100$  and  $+100^{\circ}\text{C}$ . Some ceramic materials, such as lead lanthanum zirconate titanate, exhibit the shape-memory effect.

SMA in the form of fibers may be embedded in a structural composite in order to make the composite an actuator, usually for vibration damping (active control).

A practical problem for the shape-memory effect is associated with the hysteresis during temperature cycling or stress cycling. Another problem is associated with the poor long-term stability, i.e. decrease of the effect as cycling occurs.

Applications of the shape-memory effect [5,6] include temperature-actuating and stress-actuating levers, orthodontal braces, blood clot filters and engines. Fig. 10 illustrates the use of an SMA for coupling tubing. In this application, the SMA coupling is expanded so that it fits over the tubing. Upon heating it shrinks back to its initial diameter, thereby squeezing the tubing to make a tight fit. Another application relates to the manufacture of spacecraft antennae. A wire hemisphere of a shape-memory alloy is crumbled into a tight ball. Upon subsequent heating, the ball opens up into its original shape.

In general, the use of the shape-memory effect involves the following steps: (i) betatizing (heating to equilibrate at the austenite phase field of the phase diagram), (ii) quenching to form martensite, (iii) deforming the martensite, and (iv) heating to return to the austenite phase and to restore the original shape.

A phenomenon exhibited by many SMA's below  $A_s$  is ferroelasticity, which is illustrated by the stress-strain curve in Fig. 11, which is akin to Fig. 7(a) except that no heating is involved and the stress is allowed to go negative. Tension and compression promote the growth of different variants of martensite, thus affecting the strain. This phenomenon involves plastic deformation which requires a negative stress (i.e., compressive stress) in order to eliminate. Further negative stress causes plastic deformation in the reverse direction (i.e., negative strain), which requires a positive stress (i.e., tensile stress) in order to eliminate. Thus, the stress-strain curve is a loop, which is akin to the loop in the plot of polarization vs. electric field for a ferroelectric material and to the loop in the plot of magnetic induction vs. magnetic field for a ferromagnetic

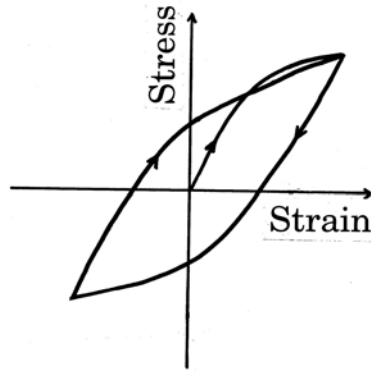


Fig. 11 Stress-strain curve for a ferroelastic material.

material. It is this similarity which causes the phenomenon of Fig. 11 to be called ferroelasticity. A ferroelastic loop has a stress plateau during tensile loading and another during compressive loading. The two plateaux provide two controlled stress levels, which can be advantageously used in actuator design.

SMA's which are ferromagnetic (e.g., Ni-Mn-Ga and Fe-Ni-Co-Ti) can be deformed in the martensite state by using a magnetic field instead of using stress [7-9]. The deformation is known as magnetoelastic deformation and usually involves re-arrangements of the martensitic twin variants.

#### References

1. Hiroyasu Funakubo, ed., Precision Machinery and Robotics, Vol. 1, Shape Memory Alloys, Gordon & Breach, New York, NY 1987
2. Z.G. Wei, R. Sandstrom and S. Miyazaki, J. Mater. Sci. 33, 3743-3762 (1998).
3. Z.G. Wei, R. Sandstrom and S. Miyazaki, J. Mater. Sci. 33, 3763-3783 (1998).
4. R. Krumme, J. Hayes and S. Sweeney, Proc. SPIE – The International Society for Optical Engineering, vol. 2445, 1995, Society of Photo-Optical Instrumentation Engineers, Bellingham, WA, p. 225-240.
5. T.W. Duerig, Materials for Smart Systems, Materials Research Society Symposium Proc., vol. 360, 1995, Materials Research Society, Pittsburgh, PA, p. 497-506.
6. J.S.N. Paine and C.A. Rogers, Adaptive Structures and Composite Materials: Analysis and Application, American Society of Mechanical Engineers, Aerospace Division, AD, vol. 45, 1994, ASME, New York, NY, p. 37-45.
7. S.J. Murray, R. Hayashi, M. Marioni, S.M. Allen and R.C. O'Handley, Proc. SPIE – the International Society for Optical Engineers, vol. 3675, 1999, Society of Photo-Optical Instrumentation Engineers, Bellingham, WA, p. 204-211.
8. V.A. Chernenko, V.A. L'vov and E. Cesari, Journal of Magnetism & Magnetic Materials 196, 859-860 (1999).
9. Y. Furuya, N.W. Hagood, H. Kimura and T. Watanabe, Materials Transactions Jim. 39(12), 1248-1254 (1998).